Colloid Polym Sci 277:957–964 (1999)

ORIGINAL CONTRIBUTION

M.R. Anklam
D.A. Saville
R.K. Prud'homme

Electric-field-induced rupture of polymer-stabilized oil films

Received: 4 February 1999
Accepted: 21 May 1999

M.R. Anklam · D.A. Saville
R.K. Prud'homme
TRI/Princeton and Department
of Chemical Engineering
Princeton University
Princeton, NJ 08544 USA

M.R. Anklam (✉)
Department of Chemical Engineering
Rose-Hulman Institute of Technology
5500 Wabash Avenue
Terre Haute, IN 47803 USA

Abstract Water-in-oil emulsions stabilized by polymeric surfactants are robust, but the reasons for their stability are poorly understood. We studied oil films stabilized by a comb–graft copolymer having a poly(siloxane) backbone and poly(ethylene oxide)/poly (propylene oxide) and C_{16} grafts (Abil EM-90) with a total number-average molecular weight of 62,000. Electric fields imposed in the aqueous phases on either side of the oil films were used to induce rapid rupture, and the response of the film was monitored using optical interference and electrical conductance measurements. Film thickness values ranged between 30 and 50 nm and rupture at field strength values between 2×10^7 and 5×10^7 V/m. Unexpectedly, in some cases, stable pores were formed and the films became electrically conductive. Often the pores persisted for more than 20 min after the voltage had been removed. Since the current was independent of film area, very few pores are involved in conduction. This behavior is similar to that found in lipid films; however, the persistence time is greater for polymer-stabilized films. Because the films are thick, it is possible that pores are formed by multimolecular self-assembly as with pore-forming proteins. Polymer purification also influenced film stability.

Key words Emulsions · Thin films · Coalescence · Graft copolymer · Electroporation

Introduction

Many water-in-oil (w/o) emulsions are stabilized by macromolecules or particulate matter when electrostatic repulsive forces are too small to provide stability. The classic method of study is to create an emulsion and to observe its behavior over a long period of time. Although this technique is useful for studies under quiescent conditions, it furnishes little information about behavior where strong mechanical forces destabilize an otherwise stable system. Dynamic studies on thin films are needed to provide insight into film stability in the presence of large stresses. One way of creating a sudden destabilizing force is to use electric fields. Since a thin oil film behaves as a capacitor when a voltage is applied, a compressional force is exerted on the film by interfacial charge. If large enough, the forces induced by the electric field cause rupture. The use of electric fields to study oil film stability is also applicable to electrical demulsification [1–4]. This paper presents a study on the rupture of polymer-stabilized oil films induced by an electric field.

Previous studies

Previous work on the electrical breakdown of oil films has focused on lipid films with applications to biomembrane studies [5–8]. Chizmadzhev and Pastushenko [9] provide a thorough review of the subject. Lipid films in an electric field experience two kinds of membrane breakdown: reversible and irreversible [6, 8]. Reversible breakdown (called electroporation) occurs when a hole develops in the membrane at a critical electric field and

heals when the voltage is removed. Irreversible breakdown (or film rupture for the case of metastable films) occurs in lipid films at sufficiently high voltages [10–17]. Longer, larger voltage pulses change reversible to irreversible breakdown [6–8, 14–16, 18].

Mechanisms of film breakdown

Two theories have been put forward for the breakdown of thin films in an electric field [9].

1. The electromechanical model [7, 19–21], which combines components from the mechanisms known as elastic breakdown [22] and hydrodynamic breakdown [23–25].
2. The pore nucleation model [9, 10, 26–29].

Elastic breakdown

In the elastic breakdown mechanism, the film is an elastic capacitor with a constant permittivity. Breakdown occurs when the voltage exceeds a critical value, V_c, where

$$V_c^2 = 0.368\frac{\Gamma h_0^2}{\varepsilon\varepsilon_o} \quad . \tag{1}$$

Here Γ is the elasticity of compression, h_0 is the thickness in the absence of an electric field, ε is the dielectric constant, and ε_o is the permittivity of free space. As discussed by Chizmadzhev and Pastushenko [9], shortcomings in the theory include the assumption of constant elasticity (despite the predicted large deformations at rupture) and the predicted large deformations at rupture despite the lack of a marked change in measured capacitances prior to rupture.

Electrohydrodynamic stability

In electrohydrodynamic breakdown [7, 20, 25] the film is a layer of nonconducting liquid with a charged, conducting fluid on either side. When analyzed for both symmetric (squeezing) and antisymmetric (stretching) perturbations, the system is found to be unstable for long-wave perturbations when

$$V_c^2 = \left(\frac{\sigma_b h}{\varepsilon\varepsilon_o}\right) \quad . \tag{2}$$

Taking into account the energy necessary to create a new interface due to the perturbations shows this is basically the same as the elastic breakdown theory.

Pore nucleation

According to the pore nucleation theory, the film is a metastable phase and rupture occurs as a phase transition when the nucleation sites (pores) reach a critical size. As this theory is discussed in detail by Chizmadzhev and Pastushenko [9], Winterhalter and Helfrich [30], and Weaver and Barnett [31], only the main concepts are presented here.

A film has many defects or pores formed naturally by thermal fluctuations. The energy of creating (or maintaining) a cylindrical pore is a balance between a (favorable) decrease in film area and an (unfavorable) increase in line tension effects (i.e., increase in internal film area in the pore). The free energy of a cylindrical pore is

$$\Delta F = -\gamma\pi r^2 + 2\pi r\kappa \ , \tag{3}$$

where r is the radius of the pore, γ is the film tension, and κ is the line tension. Thus, there will be a critical radius above which the increase in pore size is energetically favorable. The application of a voltage changes the energy of a pore. Assuming that the pores are small and nonconductive, a pore's energy is decreased at a given radius due to the higher permittivity of water such that

$$\Delta F = 2\pi r\kappa - \pi r^2\left(\gamma + \frac{\varepsilon_o(\varepsilon_w - \varepsilon_m)V^2}{2h}\right) \ , \tag{4}$$

where ε_w and ε_m are the dielectric constants of water and the membrane, respectively. So, an increase in voltage decreases the critical pore size, and larger pores form more readily due to thermal fluctuations. Wilhelm et al. [15] and Pastushenko and Chizmadzhev [32] account for effects of pore conductivity on the free energy of pore formation.

For lipid films, which are simple bilayers, the pore nucleation theory appears to be the most widely accepted. The main criticisms of the pore nucleation model are that it uses unmeasured properties to describe the process and fails to provide a mechanistic description of the origin of the instability [7]. However, the fact that current fluctuations are observed prior to film rupture [10] indicates that pore formation occurs in lipid films prior to breakdown.

Materials and methods

Film components

Abil EM-90 is a comb copolymer with a poly(dimethyl siloxane) backbone and grafted hydrophobic and hydrophilic chains as depicted in Fig. 1. The Abil surfactant was chosen because of its interesting comb–graft structure and its ability to produce remarkably stable w/o emulsions [33, 34].

Decane (99 + % Sigma) was used as the polymer solvent and 1.0 M KCl (99.99 + % Aldrich) in Picopure water was used as the aqueous phase. The solvent and salt were used as received. For all thin film experiments, the oil phase and the aqueous phase were pre-equilibrated by gently pouring the oil over the aqueous phase and allowing the phases to remain in contact for at least a week.

Abil surfactant (Goldschmidt) was purified by eight extractions with acetone to remove residual hexadecane and hexadecene (5–9%), cetyl substituted cyclic siloxanes

(1.5–1.8%), and other components, perhaps poly(ethylene oxide)/poly(propylene oxide) (0.04%) [35]. As received, Abil has a number-average molecular weight of 17,000 (from gel permeation chromatography and light scattering) and a polydispersity of 2.45; the purified product has a number-average molecular weight of 62,000 and a polydispersity of 1.2. Both purified and unpurified Abil were used in our studies.

According to capacitance measurements [36], films from the Abil surfactant are quite thick and compressible (about 40–60 nm over a 400 mV range). This thickness is about an order of magnitude larger than that for typical lipid films.

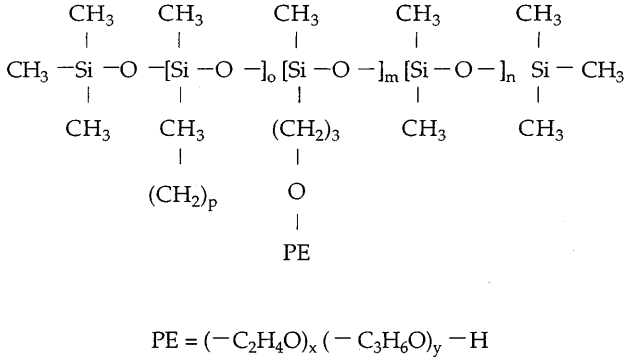

Fig. 1 Chemical structure of the Abil polymeric surfactant. The molecular weights of the various groups and the distribution are unknown

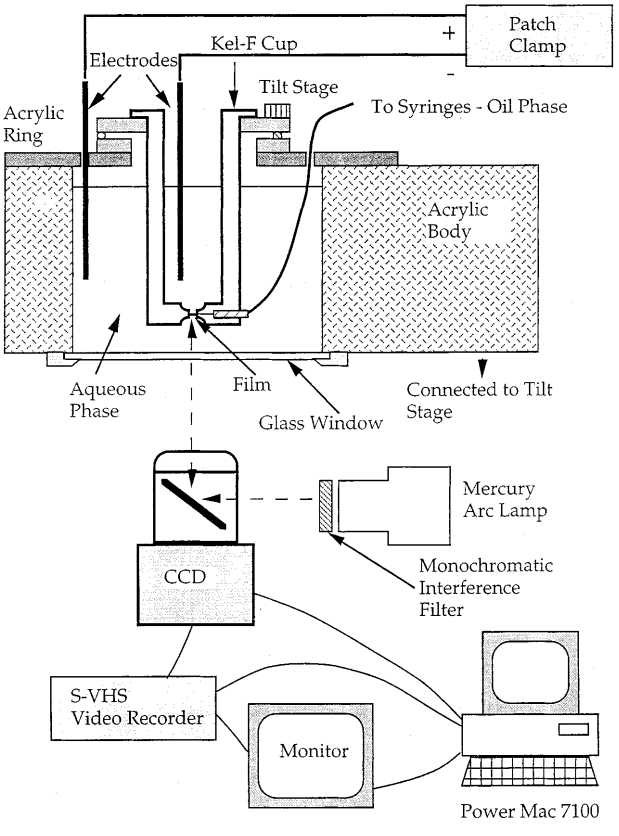

Fig. 2 Schematic showing the thin film apparatus

Thin film apparatus

The thin film apparatus (Fig. 2) is based on the design of Requena et al. [37]. A detailed description is given elsewhere [36]. The design permits simultaneous application of an electric field across the film and interferometric observation with reflected light. The design also permits the film radius to be varied by adjusting the volume of liquid in the meniscus region. The entire apparatus is surrounded by a Faraday cage and placed on a vibration isolation table.

Electronics and voltage application

A patch clamp device (Dagan 3900A integrating patch clamp with a 3901 headstage and a 3910 expander and a X10 bath connector) in voltage clamp mode was used to generate the electrical potential across the film [38–40]. Ag/AgCl electrodes were formed by electroplating following the method of Keller [38]. The use of reference Ag/AgCl electrodes connected to a high-impedance electrometer (Keithley 617) in preliminary experiments showed that the potential drop between the two aqueous phases separated by an oil film was equal to the applied voltage.

The patch clamp with the headstage permits currents up to about 13 nA. Voltages up to 500 mV may be applied in the normal operating circuit of the patch clamp; however, for film rupture experiments a X10 voltage amplifier (Dagan 3910 expander and X10 bath connector) was used to generate 5-V potentials. The patch clamp has analog outputs and inputs so current was monitored and voltage controlled on the computer via a Strawberry Tree T21 terminal panel connected to a Strawberry Tree ACM2 A/D board and Strawberry Tree's WorkbenchMac data acquisition software.

Voltage-induced rupture was studied by applying voltage ramps on a newly formed film and monitoring the electrical current until rupture. Voltage ramps of 100 mV/s were applied using external computer control. Rupture was noted visually and by a simultaneous jump in the current out of the measurable range (about 1300 pA). A jump in current for a film without signs of visible rupture was termed "leakiness" (see later).

Film formation

The experiments on film formation were begun by placing a Kel-F cup into the aqueous reservoir and pushing an excess amount of oil into the film orifice (Fig. 2). Excess oil was removed with a syringe to clear oil from the 1-mm orifice (i.e., to allow a continuous path for the aqueous phase). Oil was then slowly injected into the orifice region using the syringes until oil had filled the entire region and the aqueous phases had separated. A thin film formed upon withdrawing oil until the two interfaces came into contact. Measurements began 2 h after the interfaces had formed. The time elapsed from oil injection was designated the "age" of the experiment.

Cleaning procedure

Wetted components were washed thoroughly with detergent, rinsed exhaustively in deionized water, washed with a chromic acid/sulfuric acid solution, and finally rinsed again with deionized water.

Results and observations

When a film was exposed to a voltage ramp, several effects were observed. Typical current patterns during a voltage ramp for large (350–400-μm diameter) and small (100–150 μm) films, are shown in Fig. 3a and b respectively. Since the current increased and fluctuated

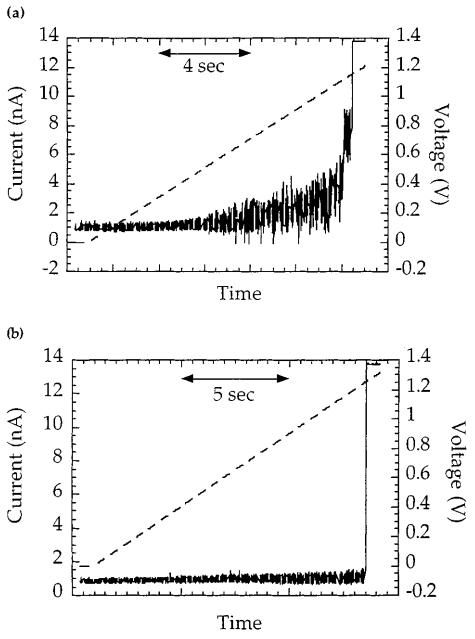

Fig. 3 Example film behavior during a voltage ramp (*dashed line*) for **a** large diameter (350–400 μm) film and **b** small diameter (100–150 μm) film from 0.52% Abil (purified) in decane

as the voltage rose during a ramp, the films did not behave as perfect insulators. At some point, the current jumped off the scale. In some cases this jump coincided with film rupture; in others the current jump occurred without film rupture (leakiness). Note that although the current due to rupture should be larger than that due to leakiness, the values are off-scale, and current–time plots look similar for the two cases. From the interference patterns, the leaky films appear to relax (i.e., lenses increase in diameter and the reflectivity increases) when the current jumps. A third type of behavior was infrequently observed during a voltage ramp: large current peaks preceded either leakiness or rupture; such behavior is not depicted here.

Film rupture was induced by voltage ramps. Measurements of film lifetime for purified and unpurified polymer are presented in Table 1. These measurements include the film lifetimes only for films which ruptured; leaky films are not included. However, the time to the onset of leakiness for the leaky films is not substantially different than the time to rupture for films that rupture. Two effects are observed. Firstly, the purified polymer gave longer film lifetimes compared to the unpurified polymer. For the purified polymer solutions, the more concentrated solutions gave more stable films. In contrast, for unpurified solutions concentration had no effect. Secondly, small-diameter films were consistently more stable than those of larger diameter; however, the statistical correlation between film size and leakiness was not explicitly studied.

Table 1 Results from rupture experiments on Abil in decane solutions using a voltage ramp of 100 mV/s. ‡ means that, for the two voltages, the upper values were obtained when the experiment "age" was only a few hours (on the first day of experiments) while the lower values were obtained when the experiment "age" was greater than 24 h (on the second day). The rupture voltage is the ramp voltage where rupture or a current jump occurred

Concentration (% w/w)	Film diameter (μm)	Median rupture voltage (V)	Mean rupture voltage (V)	Standard deviation (V)
0.058 ‡ (purified)	100–150	1.022	1.028	0.065
		1.182	1.185	0.090
	350–400	0.891	0.872	0.079
		0.967	0.924	0.185
0.52 (purified)	100–150	1.260	1.240	0.089
	350–400	1.166	1.155	0.067
0.52 (as received)	100–150	0.979	0.967	0.090
	350–400	0.864	0.844	0.074
0.058 (as received)	100–150	0.971	0.965	0.038
	350–400	0.843	0.806	0.101

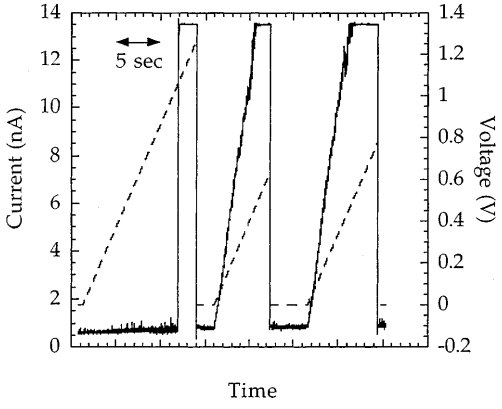

Fig. 4 Leaky film behavior with the application of a voltage ramp (*dashed line*). A fresh film experiences a jump in current at the onset of leakiness. When the ramp is repeated, the current increases linearly and strongly with voltage indicating an increased conductance. This behavior is repeatable in subsequent ramps. Measurements made on films of 0.058% Abil (purified) in decane

Unexpectedly, leaky films maintained their conductive behavior without an electric field (i.e., the pores persist once formed). The behavior of leaky films, monitored by the electrical current, for films subject to voltage ramps is shown in Fig. 4. During the initial ramp, the current followed the same pattern as with a rupture event, but when the current jumped off the scale, the film remained intact. When the voltage was removed, the current dropped to a baseline value, which was typically offset from the original zero value. Sometimes, the current displayed large fluctuations. For repeated voltage increases after the initial current jump, the current showed a strong dependence on the voltage, indicating a higher conductance and the persistence of whichever pore or path caused the initial leakiness.

Duplicate voltage ramps led to essentially identical current patterns until healing or rupture (Fig. 4). With leaky films, changes in film diameter did not significantly alter the current–voltage relation unless the film diameter was very small. Moreover, if a film was reformed after rupture of a leaky film, the reformed film did not display leaky behavior. In some cases leaky films were monitored for 15–20 min to observe long-term behavior in the absence of an applied voltage. Usually the film either ruptured or the pore(s) persisted. In a few cases (Fig. 5) leaky pores healed themselves.

Discussion

Conductivity during rupture

The behavior of leaky films varied from film to film (Figs. 4, 6, 7). The current pattern for 150-μm diameter films with different conductances is shown in Figs. 4 and 6 (Fig. 6 shows the more conductive film). With these films, the current–voltage relation is (approximately) linear. The current pattern for a 150-μm leaky film that displayed no significant increase in current until large voltages were reached is shown in Fig. 7; such behavior was rare. Comparison of conductances for leaky films with fresh, intact films provides an estimate of pore area. Conductances of films formed with 0.52 and 0.058% Abil (purified) fell in the same range, having values from 2.5×10^{-11} to 3.8×10^{-10} S for film areas of 0.11 mm^2. This corresponds to specific conductances of the order of 3×10^{-9}–3×10^{-10} S/mm^2 and conductivities of 2×10^{-10}–2×10^{-11} S/m, several orders of magnitude higher than conductivities for typical hydrocarbons (5×10^{-14} S/m) [37].

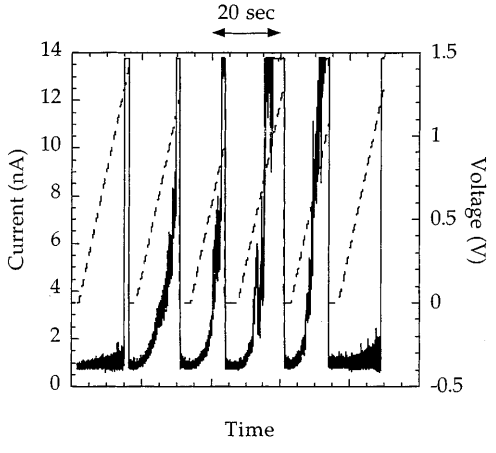

Fig. 5 Behavior of a small diameter (100–150 μm) leaky film during a voltage ramp. The voltage ramp (*dashed line*) and the resulting current display a sudden jump off the scale at the onset of leakiness. Subsequent voltage ramps show that leakiness persists. The final ramp indicates healing of the pore or hole. The film was formed from 0.52% Abil (purified) in decane solutions

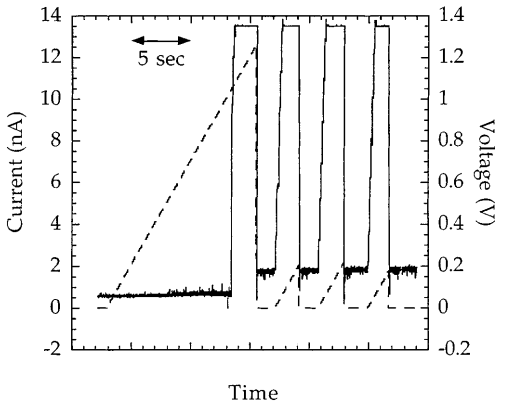

Fig. 6 Behavior of a leaky film under a voltage ramp (*dashed lines*). The initial jump in current corresponds to the onset of leaky behavior; subsequent voltage ramps show that the film is very conductive relative to most leaky films. Film – 0.058% Abil (purified) in decane

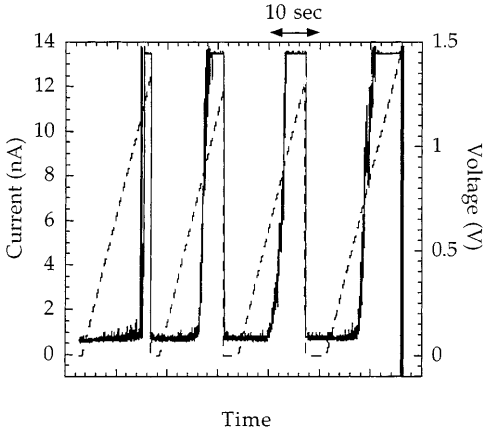

Fig. 7 Behavior of a leaky film under a voltage ramp (*dashed lines*). The current does not increase with voltage until large voltages are reached. The measurements were made using films from 0.058% Abil purified

Conductances of leaky films with approximately linear relationships between current and voltage did not appear to depend on film area, and there appeared to be no strong correlation between polymer concentration and conductance. For 0.52% Abil (purified), conductances ranged from 1.4×10^{-8} to 3.5×10^{-8} S; for 0.058% Abil (purified), conductances ranged from 2×10^{-7} to 3×10^{-8} S. Assuming that leakiness is caused by pores with a conductivity of 11 S/m (1.0 M KCl), this yields a total pore area of 150–900 nm^2. This corresponds to a single pore with a diameter less than the film thickness. According to Eq. (3), the critical pore size in the absence of an electric field is κ/γ. The line tension necessary for films of this size (about 10^{-10} J/m) would be an order of magnitude greater than line tensions calculated for lipid films (1–3×10^{-11} J/m) [40, 42]. Given that the film thickness for Abil films is an

order of magnitude greater than that for lipid films, an order of magnitude increase in line tension would not be unexpected. Note that a typical critical radius for a lipid film is about 5 nm [16]. For most of the leaky films the conductance increased slightly with voltage, suggesting an increase in pore size as voltage increases. Glaser et al. [43] showed that for lipid films the conductivity is a strong function of voltage and that pores typically form with an opening of 0.5–1.0 nm. For most of the Abil films, conductance does not change significantly and does not approach zero as the voltage approaches zero. It appears that only a few pores are present and that they remain intact as the voltage drops.

Number of pores

How many pores are formed? For lipid films, this is the subject of debate. Some results suggest that a large number of pores are present and lead to reversible breakdown [8, 44, 45]; other results suggest very few pores are involved in rupture [15, 16]. Our observations on Abil films suggest that only a few pores, possibly only one, are responsible for the leaky behavior. Should a great number of pores be present, the conductance would be expected to be proportional to film area; however, the conductance of the leaky films did not depend on the initial film diameter and did not change when film diameter was decreased. It should also be noted that leaky behavior did not continue when the film diameter was decreased to zero, indicating that the conductive path was indeed within the film rather than elsewhere (e.g., where the meniscus meets the solid wall). It was also observed that the leaky film behavior was reproducible (Fig. 4). Multiple pores would be expected to have varying healing rates. So, as pores heal, the conductances would decrease for subsequent voltage ramps. In all but a few cases, films extant after a current jump behaved in a leaky manner (increased conductance) during subsequent voltage ramps.

Rupture and leakiness

The distinction between electrically induced leakiness and rupture depends on the applied voltage. Two types of pores are formed during the voltage ramp. Before the onset of irreversible leakiness, current fluctuations were observed (Figs. 3, 8). These may be likened to random pores growing to a subcritical, but substantial, size and then shrinking under thermal fluctuations. The noise from the external computer connection and the X10 voltage amplifier prevented any statistical analyses of the fluctuations. A more permanent pore structure (albeit a rather unstable one) was observed at higher electric fields or longer ramp times. These pores either persisted or led to film rupture.

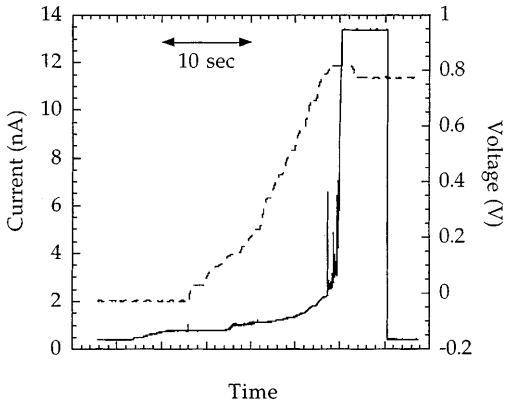

Fig. 8 Film behavior during a manually controlled voltage increase (*dashed curve*) using the patch clamp. Significant noise reduction is observed compared with automatically controlled ramps (e.g., Fig. 3). Only a few current fluctuations are present prior to rupture (current jump). The measurements were made using a film from 0.52% Abil (purified) in decane

Our observations are analogous to those of pore formation in biological membranes and lipid films. The rates of pore healing reported in the literature vary widely, depending on the system; healing times range from 1 s [6, 16, 18] to significantly longer [43, 46]. Work on pore lifetimes [8, 43, 46] shows that the rate of healing is dependent on the voltage pulse size and duration; very long lived pores (with ages exceeding 30 min) can be obtained with biomembranes. Pore lifetimes in lipid films are somewhat shorter but still range from seconds to minutes. Presumably the difference is caused by the membrane proteins and channels associated with the biomembranes. An exception is the long-lived pore (the so-called stressed state) observed in lipid films by Abidor and coworkers [10, 47] These authors suggest that the persistence of a pore may be due to an energy activation barrier. This is easily overcome when the voltage is applied but is more difficult to surmount when the voltage is removed (e.g., the rearrangement of surfactant to cover the interior interface as shown in Fig. 9). Reversible and irreversible breakdowns for lipid films occur under different conditions of voltage pulse amplitude and duration [6, 8], and the two types of breakdown are not the same at a given stress. In our work, reversible and irreversible breakdown did occur under seemingly identical conditions.

The mechanism of pore formation

The fact that the jump in current led to leakiness or rupture implies that pore formation and growth leads to film rupture. As mentioned earlier, a current jump can be interpreted as the growth of a pore leading to either a stable configuration or instability when the voltage

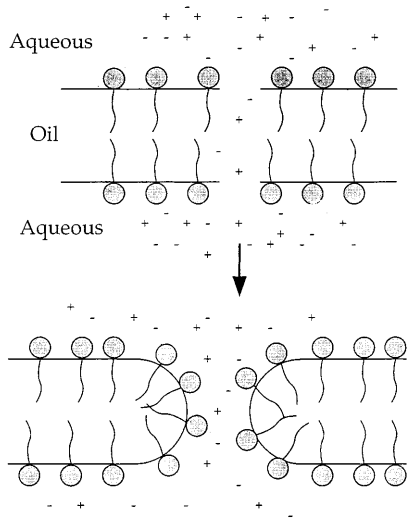

Fig. 9 Transformation of a straight or hydrophobic pore to a hydrophilic one where the surfactant molecules cover the inside of the pore. This rearrangement requires an activation energy barrier to be overcome, and thus may explain the persistence of pores

drops. That pore growth leads to rupture would explain why leaky pores can be observed. The unanswered question is how pores form.

Abil films are quite thick. Moreover, in a dilute solution the hydrodynamic radius of the polymer particle or aggregate is about 6 nm [36]. Such aggregates would consist of an ethylene oxide core in a reverse-micelle-like structure. Although the exact structure of the polymer within the film is not known, one possibility is an arrangement or network of layers of loosely connected aggregates. With the application of an electric field, these aggregates may behave like electrorheological fluids or pore-forming proteins. Thus, similar to particles in an electrorheological fluid, the polymer aggregates may form chains. At high voltages, such bridging leads to increased conductance. Alternatively, Abil molecules may rearrange so that ethylene oxide and propylene oxide groups orient themselves inwards to form a conductive path. This behavior is similar to that of pore-forming proteins which assemble to form a conducting pore with interior hydrophilic and exterior hydrophobic regions [38, 48–50].

Summary and Conclusions

Electric-field-induced rupture experiments were performed on oil films stabilized with a comb–graft copolymer having a poly(siloxane) backbone and poly(ethylene oxide)/poly(propylene oxide) and C_{16} grafts (Abil EM-90). Typically, film rupture occurred at field strengths between 2×10^7 and 5×10^7 V/m. Film diameter and polymer purification were found to significantly influence film stability. In some cases the films became conductive at these field strengths, yet remained intact. From current measurements, pore areas of 150–900 nm^2 were estimated. Since the current did not depend on total film area, a single pore or very few pores are involved. The pore-forming structures are persistent, typically lasting longer than 15 min. This is similar to pore formation in lipid films although the persistence time scale appears to be greater for polymer-stabilized films. The length scale (30–50-nm thick films) and persistence suggest that the pore is formed by a multimolecular process similar to those with pore-forming proteins. This is the first example of electrically induced pore formation for synthetic graft copolymers.

Acknowledgements We would like to acknowledge financial support from TRI/Princeton, helpful discussions about pore formation in lipid films with Adrian Parsegian at NIH, and Sol Gruner of Cornell University for the use of the patch clamp electronics.

References

1. Waterman LC (1965) Chem Eng Prog 61:51
2. Hauertmann HB, Degener W, Schugerl K (1989) Sep Sci Technol 24:253
3. Taylor SE (1988) Colloids Surf 29:29
4. Mohammed RA, Bailey AI, Luckham PF, Taylor SE (1993) Colloids Surf A 80:223
5. Weaver JC (1994) In: Lee RC, Capelli-Schellpfeffer M (eds) Electrical injury: a multidisciplinary approach to therapy, prevention, and rehabilitation, vol 720. New York Academy of Sciences, New York, p 141
6. Zimmermann U (1982) Biochim Biophys Acta 694:227
7. Dimitrov DS, Jain RK (1984) Biochim Biophys Acta 779:437
8. Chernomordik LV, Chizmadzhev YA (1989) In: Neumann E, Sowers AE, Jordan CA (eds) Electroporation and electrofusion in cell biology. Plenum, New York, p 83
9. Chizmadzhev YA, Pastushenko VF (1988) In: Ivanov IB (ed) Thin liquid films: fundamentals and applications. Dekker, New York, p 1059
10. Abidor IG, Arakelyan VB, Chernomordik LV, Chizmadzhev YA, Pastushenko VF, Tarasevich MR (1979) Bioelectrochem Bioenerg 6:37
11. Melikyan GB, Matinyan NS, Kocharov SL, Arakelian VB, Prangishvili DA, Nadareishvili KG (1991) Biochim Biophys Acta 1068:245
12. Bulavchenko AI, Kruglyakov PM (1984) Kolloidn Zh 46:408
13. Sukharev SI, Arakelyan VB, Abidor IG, Chernomordik LV, Pastushenko VF (1983) Biophysics (USSR) 28:801
14. Chernomordik LV, Sukharev SI, Abidor IG, Chizmadzhev YA (1983) Biochim Biophys Acta 736:203
15. Wilhelm C, Winterhalter M, Zimmermann U, Benz R (1993) Biophys J 64:121

16. Winterhalter M, Klotz KH, Benz R, Arnold WM (1996) IEEE Trans Ind Appl 32:125
17. Klotz KH, Winterhalter M, Benz R (1993) Biochim Biophys Acta 1147: 161
18. Benz R, Zimmermann U (1981) Biochim Biophys Acta 640:169
19. Zimmermann U, Pilwat G, Pequeux A, Gilles R (1980) J Membr Biol 54: 103
20. Maldarelli C, Jain RK (1988) In: Ivanov IB (ed) Thin liquid films: fundamentals and applications. Dekker, New York, p 497
21. Dimitrov DS (1984) J Membr Biol 78:53
22. Crowley JM (1973) Biophys J 13:711
23. Michael DH, Norbury J, O'Neill ME (1974) J Fluid Mech 66:289
24. Michael DH, Norbury J, O'Neill ME (1975) J Fluid Mech 72:95
25. Michael DH, O'Neill ME (1970) J Fluid Mech 41:571
26. Pastushenko VF, Chizmadzev YA, Arakelyan VB (1979) Bioelectrochem Bioenerg 6:53
27. Derjaguin BV, Gutop YV (1962) Kolloidn Zh 24:431
28. Chizmadzhev YA, Chernomordik LV, Pastushenko VF, Abidor IG (1982) In: Biophysics of membranes. Results of science and engineering, vol 2. All-Union Institute of Scientific and Technical Information, Moscow, p 161
29. Kashchiev D, Exerowa D (1980) J Colloid Interface Sci 77:501
30. Winterhalter M, Helfrich W (1987) Phys Rev A 36, 5874
31. Weaver JC, Barnett A (1992) In: Chang DC, Chassy BM, Saunders JA, Sowers AE (eds) Guide to electroporation and electrofusion. Academic Press, San Diego, p 91
32. Pastushenko VF, Chizmadzhev YA (1982) Gen Physiol Biophys 1:43
33. Garti N, Aserin A (1996) Adv Colloid Interface Sci 65:37
34. Sela Y, Magdassi S, Garti N (1994) Colloids Surf A 83:143
35. Personal Communication with M. Long at Helene-Curtis 1996
36. Anklam MR, Saville DA, Prud'homme RK (1999) Langmuir (in press)
37. Requena J, Billett DF, Haydon DA (1975) Proc R Soc Lond Ser A 347:141
38. Keller SL (1995) PhD thesis. Princeton University
39. Sakmann B, Neher E (eds) Single-channel recording. Plenum, New York
40. Rudy B, Iverson LE (eds) Ion channels, vol 207. Academic Press, San Diego
41. Chernomordik LV, Melikyan GB, Chizmadzhev YA (1987) Biochim Biophys Acta 906:309
42. Genco I, Gliozzi A, Relini A, Robello M, Scalas E (1993) Biochim Biophys Acta 1149:10
43. Glaser RW, Leikin SL, Chernomordik LV, Pastushenko VF, Sokirko AI (1988) Biochim Biophys Acta 940:275
44. Benz R, Beckers F, Zimmermann U (1979) J Membr Biol 48:181
45. Chang DC, Saunders JA, Chassy BM, Sowers AE (1992) In:Chang DC, Chassy BM, Saunders JA, Sowers AE (eds) Guide to electroporation and electrofusion. Academic Press, San Diego, p 1
46. Chernomordik LV, Sukharev SI, Popov SV, Pastushenko VF, Sorkirko AV, Abidor IG, Chizmadzhev YA (1987) Biochim Biophys Acta 902:360
47. Chernomordik LV, Abidor IG (1980) Bioelectrochem Bioenerg 7:617
48. Ring A (1992) Biophys J 61:1306
49. Bayley H (1995) Bioorg Chem 23:340
50. Reynaud JA, Sy D (1994) Bioelectrochem Bioenerg 34:1